Enhancing the performance of a bistable energy harvesting device via the cross-entropy method

Americo Cunha Jr

Enhancing the Performance of a Bi-stable Energy Harvesting Device via Cross-entropy Method

A. Cunha Jr[1]

[1]Universidade do Estado do Rio de Janeiro, NUMERICO – Nucleus of Modeling and Experimentation with Computers, email: americo@ime.uerj.br

ABSTRACT

This work deals with the formulation and numerical solution of a nonlinear optimization problem, with discontinuous constraint, in the context of energy harvesting. This optimization problem, which seeks to find a suitable configuration of parameters that maximize the electrical power recovered by a bi-stable energy harvesting device, is formulated in terms of the harvesting dynamical system response and a classifier obtained from 0-1 test for chaos. A stochastic strategy of solution, combining penalization and cross-entropy (CE) method is proposed and tested numerically. The results illustrate the effectiveness of the proposed optimization strategy when compared to a reference solution obtained with a standard exhaustive search in a very fine grid.

1 INTRODUCTION

Energy harvesting is a process in which a certain amount of energy is pumped from an abundant source (solar, wind, ocean, environmental vibrations, electromagnetic radiation, etc) into another system that stores and/or use this energy for its own operation (Priya and Inman, 2009; Spies et al., 2015). The field of applicability of this technology ranges from large-scale generation to the use in small devices such as sensors (Bhatti et al., 2016), medical implants (Pfenniger et al., 2014), micro electro-mechanical systems - MEMS (Nabavi and Zhang, 2016), nano electro-mechanical systems - NEMS (Selvan and Ali, 2016), etc.

Enhance the amount of energy collected by energy harvesting devices is a key problem in the operation of these dispositives, being the object of interest of several recent research works (Harne, 2012; Rechenbach et al., 2016; Ying et al., 2015; Peterson et al., 2016; Lopes et al., 2017). In this sense, this work seeks to find a strategy to increase the performance of a harvesting device. For this purpose, a nonlinear optimization problem with discontinuities is formulated, and a stochastic approach to construct an approximation for the solution, based on the *cross-entropy (CE) method* (Rubinstein, 1997; Rubinstein and Kroese, 2004; Kroese et al., 2013), is proposed and numerically tested.

The rest of this manuscript is organized as follows. Section 2 presents the physical device of interest and the underlying dynamical system. An optimization problem associated to this dynamical system, and stochastic strategy of solution are defined in the section 3. Numerical experiments, conducted to test the effectiveness of solution strategy, are shown in section 4. Finally, in section 5, final remarks are set out.

2 NONLINEAR DYNAMICAL SYSTEM

2.1 Physical system

The energy harvesting system of interest in this work, proposed by (Erturk et al., 2009), is the piezo-magneto-elastic device illustrated in Figure 1. It consists in a vertical fixed-free beam made of ferromagnetic material, a rigid base and a pair of magnets. In the beam upper part there is a pair of piezoelectric laminae coupled to a resistive circuit. The rigid base is periodically excited by a force, which, together with the magnetic force generated by magnets, induces large amplitude vibrations. The piezoelectric laminae convert the energy of movement into electrical power, which is dissipated in the resistor.

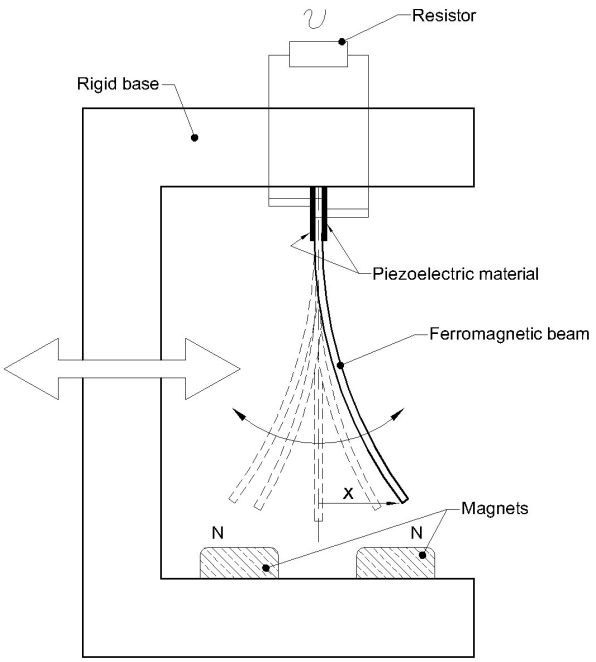

Figure 1. Illustration of the piezo-magneto-elastic energy harvesting device of (Erturk et al., 2009).

2.2 Initial value problem

As shown in (Erturk et al., 2009), the dynamic behavior of the system of interest is described by the following initial value problem

$$\ddot{x} + 2\,\xi\,\dot{x} - \frac{1}{2}x\left(1 - x^2\right) - \chi\,v = f\,\cos\left(\Omega\,t\right), \tag{1}$$

$$\dot{v} + \lambda\,v + \kappa\,\dot{x} = 0, \tag{2}$$

$$x(0) = x_0,\ \dot{x}(0) = \dot{x}_0,\ v(0) = v_0, \tag{3}$$

where ξ is the damping ratio; χ is the piezoelectric coupling term in mechanical equation; λ is a reciprocal time constant; κ is the piezoelectric coupling term in electrical equation; f is the rigid base oscillation amplitude; Ω is the external excitation frequency. All of these parameters are positive. The initial conditions are x_0, $\dot{x}_0$ and v_0 which respectively represent, the beam edge initial position, initial velocity and the initial voltage over the resistor. In addition, t denotes the time, so that the beam edge displacement at time t is given by $x(t)$, and the resistor voltage at t is represented by $v(t)$. The upper dot is an abbreviation for time derivative, and all of these parameters are dimensionless.

2.3 Output mean power

In this document the main quantity of interest (QoI) associated to the nonlinear dynamical system under analysis is the output power

$$P = \frac{1}{T}\int_{\tau=0}^{T} \lambda\,v^2(\tau)\,d\tau, \tag{4}$$

defined as the temporal average of instantaneous power $\lambda\,v^2$ over time interval $[0, T]$.

2.4 Dynamical system classifier

Due to dynamical system nonlinearity, the harvesting device steady state dynamics may be chaotic or regular (non-chaotic), such as illustrated in Figure 2, which show voltage time series.

In order to distinguish between the chaotic and regular dynamics, the 0-1 test for chaos by (Gottwald and Melbourne, 2004, 2009a,b, 2016) is employed. This test, which is based on a extension of the dynamical system to a two-dimensional Euclidean group (Bernardini and Litak, 2016), uses a binary classifier K to identify the regime of the dynamics. This classifier is constructed from a time observable $\phi(t)$. In fact, it is sufficient to use $\mathbf{\Phi} = \big(\phi(t_1), \phi(t_2), \cdots, \phi(t_N)\big)$, a discrete version of the observable $\phi(t)$ that is obtained through a sampling process (numerical integration procedure).

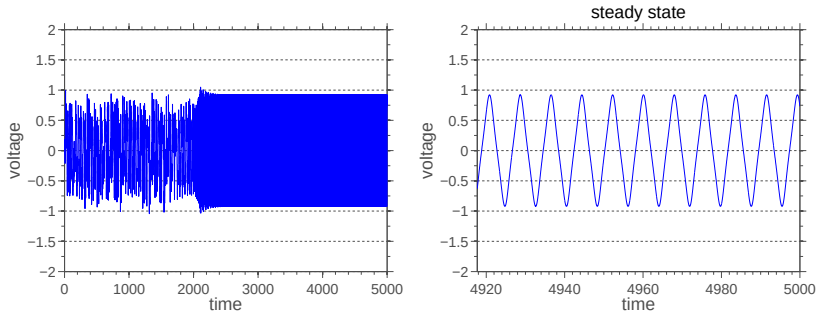

(a) regular dynamics

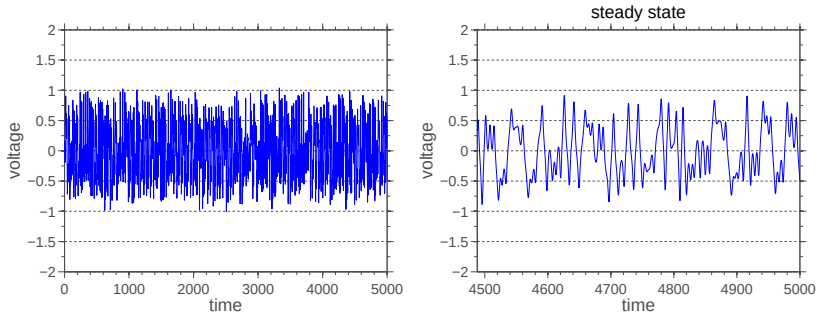

(b) chaotic dynamics

Figure 2. Two typical time series of voltage for the harvesting device. The time series in (a) has regular steady-state dynamics, while in (b) chaotic steady-state dynamics is observed.

Receiving this discrete observable as input, test 0-1 analytical procedure consists of the following steps:

1. A real parameter $c \in [0, 2\pi)$ is chosen, and the discrete version of $\phi(t)$ is used to define the translation variables

$$p_n(c) = \sum_{j=1}^{n} \phi(t_j) \cos(j\,c), \quad \text{and} \quad q_n(c) = \sum_{j=1}^{n} \phi(t_j) \sin(j\,c), \tag{5}$$

   for $n = 1, 2, \cdots, N$.

2. Then the time-averaged mean square displacement of the dynamics trajectory in (p_c, q_c) space is computed by

$$M_n(c) = \lim_{N\to\infty} \frac{1}{N} \sum_{j=1}^{N} \left(\left[p_{j+n}(c) - p_j(c)\right]^2 + \left[q_{j+n}(c) - q_j(c)\right]^2 \right), \tag{6}$$

   for $n = 1, 2, \cdots, N$.

3. Finally, defining $\mathbf{M}_n = (M_1, M_2, \cdots, M_n)$ and $\mathbf{t}_n = (t_1, t_2, \cdots, t_n)$, the classifier of the dynamics is constructed through the correlation

$$K_c = \lim_{n\to\infty} \frac{\mathtt{cov}\,(\mathbf{t}_n, \mathbf{M}_n)}{\sqrt{\mathtt{var}\,(\mathbf{t}_n)\ \mathtt{var}\,(\mathbf{M}_n)}}, \tag{7}$$

where $\mathtt{cov}\,(\cdot,\cdot)$ and $\mathtt{var}\,(\cdot)$ respectively denote the covariance and variance operators.

It can be proved that $K_c \in \{0, 1\}$, being $K_c = 0$ for regular dynamics and $K_c = 1$ for chaotic dynamics (Gottwald and Melbourne, 2009b; Bernardini and Litak, 2016).

For numerical implementation purposes, the above procedure is performed several times, for many values of c randomly chosen and $\phi(t) = v(t)$, with discrete version constructed through temporal integration via Runge-Kuta method. The limit processes in Eqs.(6) and (7) are replaced by the condition $n \ll N$, and the classifier K is calculated as the median of K_c realizations, i.e., $K = \mathtt{median}\,(K_c)$. Indeed, for a careful done numerical simulation one has $K \approx 0$ or $K \approx 1$. See (Gottwald and Melbourne, 2009a) for further details.

3 NONLINEAR OPTIMIZATION PROBLEM

The objective of this work is to find a setting of parameter that maximize the mean power P into the resistor. For this, it is more natural try to vary the parameters f and Ω, which are related to the periodic force (system input), once their are easier to be controlled than the others (which are related to the system physical characteristics).

However, not every pair (f, Ω) is an acceptable choice, since many combinations of then lead the dynamical system to operate in chaotic regime, an undesirable condition for electric power usage. This makes necessary to impose the constraint which ensures that system dynamics is regular. Taking advantage of 0-1 test for chaos, described in section 2.4, the constraint to ensure a regular (non-chaotic) dynamic regime can be formulated as $K = 0$. Note that the optimization problem is extremely nontrivial, since $K \in \{0, 1\}$ the constraint presents jump-type discontinuities.

3.1 Constrained problem

The constrained optimization problem mentioned above can be formalized as find the pair $(f^\star, \Omega^\star)$ such that

$$(f^\star, \Omega^\star) = \arg \max_{(f,\Omega)\in\mathcal{D}_{adm}} P(f, \Omega). \tag{8}$$

where the set of admissible (feasible) parameters is defined as

$$\mathcal{D}_{adm} = \left\{(f, \Omega) \mid f_{min} \le f \le f_{max},\ \Omega_{min} \le \Omega \le \Omega_{max},\ K = 0\right\}. \tag{9}$$

3.2 Penalized problem

A penalized version of the constrained optimization problem is introduced here in order to facilitate the computational implementation of the solution algorithm. In this formulation the constraint $K = 0$ is replaced by the weaker condition $K \leq \varepsilon \ll 1$, once in practice the best one has is $K \approx 0$. In this way, the problem defined by (8) is replaced by the penalized problem which seeks a pair $(f_\alpha^\star, \Omega_\alpha^\star)$, parametrized by the penalty parameters α, such that

$$(f_\alpha^\star, \Omega_\alpha^\star) = \arg \max_{(f,\Omega)\in\mathcal{D}'_{adm}} \left\{ P(f,\Omega) \, - \, \alpha \, \max\left\{0, K \, - \, \varepsilon\right)\right\}\Big\}. \tag{10}$$

where the set of feasible parameters is now defined as

$$\mathcal{D}'_{adm} = \left\{(f,\Omega) \mid f_{min} \leq f \leq f_{max},\, \Omega_{min} \leq \Omega \leq \Omega_{max}\right\}. \tag{11}$$

The penalty parameter is heuristically obtained, being $\alpha = 10$ the value used in all simulations reported in this work. In the same way, $\varepsilon = 1/10$ is chosen.

3.3 Cross-entropy strategy of solution

In an abstract way, one can see the penalized optimization problem defined in section 3.2 as find a vector $\mathbf{x}$ that maximize a certain cost function $\mathcal{S}(\mathbf{x})$. For a global optimal $\mathbf{x}^\star$ one has $\gamma^\star = \max \mathcal{S}(\mathbf{x}^\star)$. In the CE method the vector $\mathbf{x}$ is randomized and the optimization problem above is associated to the rare-event probability

$$\mathcal{P}\left\{\mathcal{S}(\mathbf{X}) \geq \gamma\right\} = \mathbb{E}\left\{\mathbb{1}_{\left\{\mathcal{S}(\mathbf{X})\geq\gamma\right\}}\right\} \;\text{ for }\; \gamma \approx \gamma^\star, \tag{12}$$

where $\mathbb{E}\left\{\cdot\right\}$ is the expected value operator, $\mathbb{1}_{\mathcal{A}}$ is the indicator function of event $\mathcal{A}$, and $\mathbf{X}$ is a random vector with probability density function $f\left(\mathbf{x};\mathbf{v}\right)$, parametrized by $\mathbf{v}$. The idea of CE method is generates a sequence of estimators $\left(\widehat{\gamma}_t, \widehat{\mathbf{v}}_t\right)$ such that $\widehat{\gamma}_t \xrightarrow{a.s.} \gamma^\star$ and $f\left(\mathbf{x}, \widehat{\mathbf{v}}_t\right) \xrightarrow{a.s.} \delta\left(\mathbf{x} - \mathbf{x}^\star\right)$, i.e., the family of distributions $f(\cdot\,,\,\mathbf{v})$ tends towards a point mass distribution, centered on a global optimum for the optimization problem. This sequence of estimators is optimal in the sense that it minimize the Kullback-Leibner divergence between $\mathbb{1}_{\left\{\mathcal{S}(\mathbf{X})\geq\gamma\right\}}$ and $f(\cdot\,,\,\mathbf{v})$.

The CE algorithm can be summarized as follows: (i) Define the number of samples N^s, the number of elite samples N^e, a convergence tolerance `tol`, the maximum of levels t_{max}, a family of probability distributions $f\left(\cdot,\mathbf{v}\right)$, an initial vector of parameters $\widehat{\mathbf{v}}_0$ for f and set the level counter $t = 0$; (ii) Update level $t = t + 1$; (iii) Generate $\mathbf{X}_1, \cdots, \mathbf{X}_N$ (iid) samples from $f\left(\cdot, \widehat{\mathbf{v}}_{t-1}\right)$; (iv) Evaluate performance function $\mathcal{S}(\mathbf{X}_n)$ at samples $\mathbf{X}_1, \cdots, \mathbf{X}_N$ and sort the results $\mathcal{S}_{(1)} \leq \cdots \leq \mathcal{S}_{(N)}$; (v) Update estimators $\widehat{\gamma}_t$ and $\widehat{\mathbf{v}}_t$; (vi) Repeat (ii) — (v) while a stopping criterion is not met. Further details can be seen in (Rubinstein and Kroese, 2016; Kroese et al., 2011; De Boer et al., 2005; Rubinstein and Kroese, 2004).

4 NUMERICAL EXPERIMENTS

For the numerical experiments conducted here, the following numerical values are adopted for the model parameters: $\xi = 0.01$, $\chi = 0.05$, $\kappa = 0.5$ and $\lambda = 0.05$. The initial condition is defined by $x_0 = 1$, $\dot{x}_0 = 0$ and $v = 0$. The dynamics is integrated over the time interval $[t_0, t_f] = [0, 2500]$, and the average output power is computed over the last 50% of this time series.

4.1 Reference solution

In order to analyze the effectiveness of the stochastic strategy of solution proposed here, a reference solution is calculated by a standard exhaustive search on fine grid over the domain

$$\mathcal{D}'_{adm} = \left\{ (f, \Omega) \,|\, 0.08 \leq f \leq 0.1,\ 0.75 \leq \Omega \leq 0.85 \right\}.$$

In this standard approach, a 256 x 256 structured uniform grid is used to discretize $\mathcal{D}'_{adm}$. System dynamics is integrated for each grid point, with the restriction being evaluated next. The objective function is evaluated at all feasible points, and the extreme value is updated at each step of the grid scanning process. Two contour maps, associated to the reference solution, are shown in Figure 3: (a) constraint function, and (b) objective function. The pair $(f, \Omega) = (0.0994, 0.7771)$ that corresponds to the global maximum is indicated in both contour maps by a red cross, being associated with an averaged power value $P = 0.3438$. Figure 4 shows a magnification of the global maximum neighborhood, where it is possible to better appreciate the contour levels shape, and verify that it actually corresponds to regular dynamics configuration. For reference, this solution was obtained in 14 hours in a MacBook Pro "Core i7" 2.2 GHz 16GB 1333 MHz DDR3.

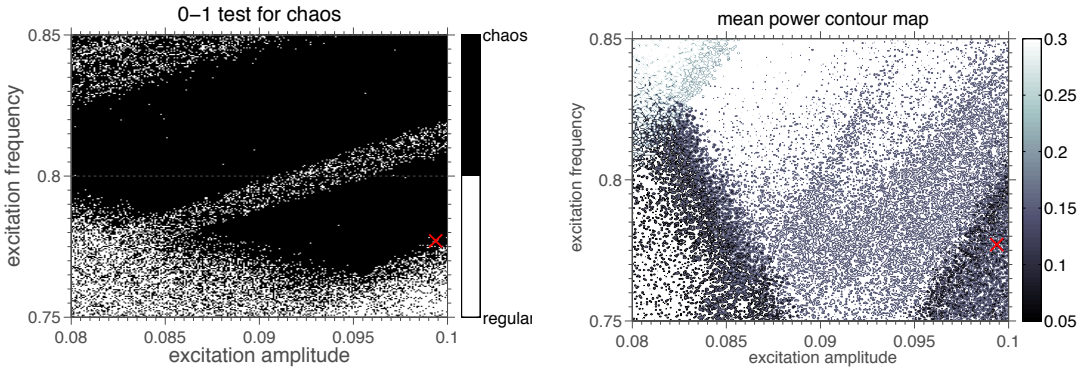

(a) (b)

Figure 3. Contour maps of: (a) constraint function defined by 0-1 test for chaos, and (b) objective function defined by average output power.

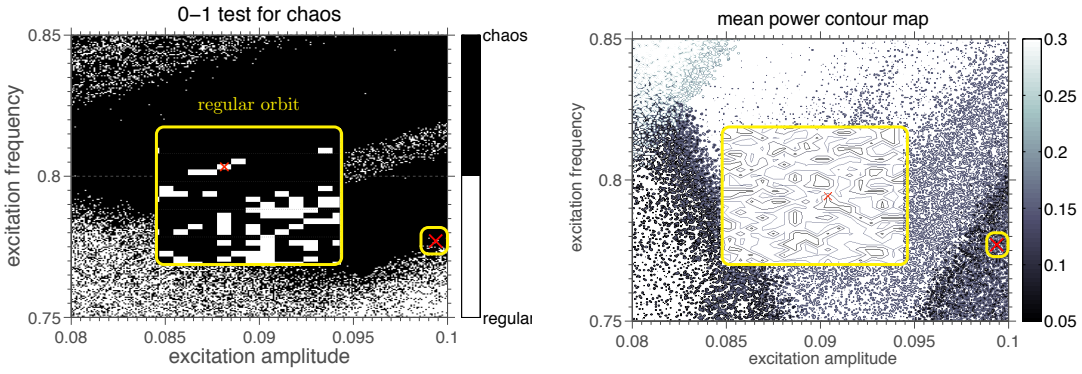

(a) (b)

Figure 4. Magnification of the contour maps around the global maximum: (a) constraint function, and (b) objective function.

4.2 Cross-entropy solution

In the approach based on the CE method, the domain is randomly sampled using for this $N^s = 50$ points. This sampling is done according to a truncated Gaussian distribution, parametrized by mean vector $\boldsymbol{\mu} = (\mu_f, \mu_\Omega)$ and standard deviation vector $\boldsymbol{\sigma} = (\sigma_f, \sigma_\Omega)$. The number of elite samples is chosen as $N^e = \texttt{round}(N^s/10)$, maximum number of levels is set $t_{max} = 100$, while the convergence criterion is adopted as $\max\left(\sigma_f, \sigma_\Omega\right) < \texttt{tol}$, for tolerance $\texttt{tol} = 1 \times 10^{-3}$.

A visual illustration of the CE method is presented in Figure 5, which shows the domain sampling at different levels (iterations) of the algorithm. An animation of the algorithm in action is available at `https://youtu.be/-JB3eniIdDY`. The reader can also appreciate the evolution of this random algorithm in Table 1, where each line displays the level index, the value of the means[1] and standard deviations of f and Ω in addition to the optimal value obtained for the objective function P.

Note that the approximation obtained is very close to the reference value of section 4.1, obtained after 17 iterative steps only, which corresponds to a speed-up of more than 70, when compared with the exhaustive search (see in Table 2 the CPU time spent). The accuracy can still be slightly improved as shown in Table 3, which presents the CE results with $N^s = 75$. The corresponding animation can be seen in `https://youtu.be/uIZM4SjCbrw`. The price to be paid for this additional gain of accuracy is a lost of performance, which makes the speed-up fall from more than 70 to 29 (see Table 2). An experiment with only $N^s = 25$ samples is also conducted (see `https://youtu.be/0EvzdVXlPqA`), obtaining a result with no significant loss of accuracy and more than doubling the speed-up to an impressive value of 167.

[1]Remember that the approximation of the optimum point is given by the vector of means, i.e., $(\mu_f^*, \mu_\Omega^*) \approx (\mu_f, \mu_\Omega)$.

The above results allow us to conclude that optimization approach based on CE method is very robust and efficient to address this nonlinear problem, which has non-trivial numerical solution, since the existence of jump-like discontinuities in the constraint prevents gradient-based algorithms from being used.

These impressive results can still be improved in terms of performance, through the use of parallelization strategies. In particular, it would be interesting to test the cloud computing parallelization strategy proposed by (Cunha Jr et al., 2014).

Table 1. Evolution of CE algorithm using $N^s = 50$ samples.

level	P	μ_f	μ_Ω	σ_f	σ_Ω
01	+7.2903E-03	+8.7521E-02	+7.9356E-01	2.5169E-02	1.2591E-01
02	+6.3452E-03	+9.1001E-02	+7.7788E-01	1.0063E-02	4.8201E-02
03	-9.7244E-01	+9.2414E-02	+7.6584E-01	7.1447E-03	2.0125E-02
04	+7.7948E-03	+9.5157E-02	+7.5804E-01	4.1197E-03	1.0032E-02
05	+3.3424E-01	+9.6867E-02	+7.6026E-01	2.8178E-03	5.7698E-03
06	+3.3530E-01	+9.7061E-02	+7.6248E-01	1.9266E-03	4.2519E-03
07	+3.3726E-01	+9.7527E-02	+7.6526E-01	1.7550E-03	3.3838E-03
08	+3.3792E-01	+9.8206E-02	+7.6673E-01	1.6807E-03	2.4310E-03
09	+3.3854E-01	+9.8699E-02	+7.6805E-01	1.4523E-03	2.4036E-03
10	+3.3990E-01	+9.8556E-02	+7.6977E-01	1.1245E-03	1.9528E-03
11	+3.4022E-01	+9.8770E-02	+7.7115E-01	9.7944E-04	1.6709E-03
12	+3.4083E-01	+9.8589E-02	+7.7247E-01	9.5384E-04	1.4976E-03
13	+3.4155E-01	+9.8756E-02	+7.7361E-01	8.2175E-04	1.3074E-03
14	+3.4126E-01	+9.9368E-02	+7.7329E-01	6.9106E-04	1.1287E-03
15	+3.4143E-01	+9.9423E-02	+7.7342E-01	6.2239E-04	1.1614E-03
16	+3.4115E-01	+9.9543E-02	+7.7319E-01	6.0541E-04	1.1051E-03
17	+3.4191E-01	+9.9790E-02	+7.7392E-01	4.9657E-04	9.6386E-04

Table 2. Performance of CE algorithm for different number of samples.

samples	levels	CPU time* (seconds)	speed-up
reference	—	50 632	—
25	15	304	167
50	17	696	73
75	29	1736	29

*MacBook Pro “Core i7" 2.2 GHz 16GB 1333 MHz DDR3

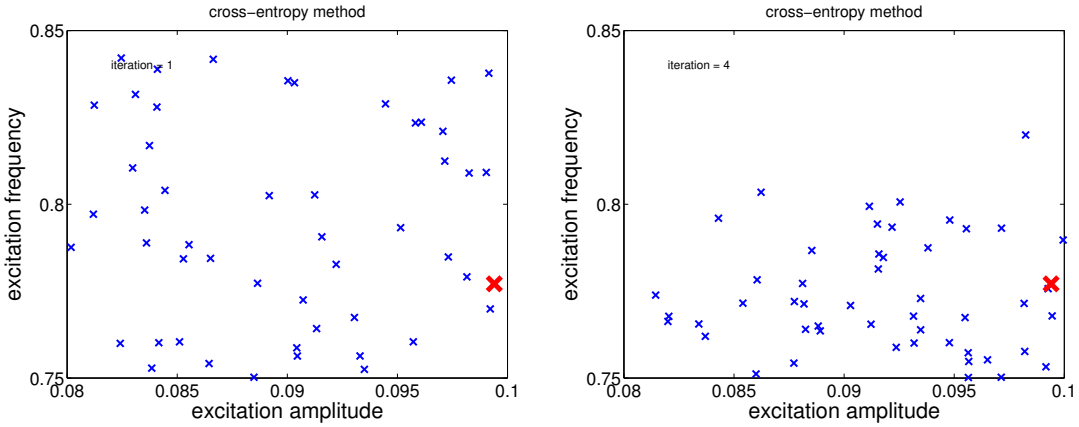

(a) $t = 1$

(b) $t = 4$

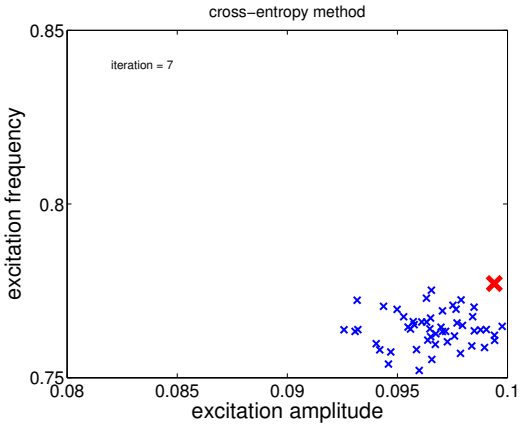

(c) $t = 7$

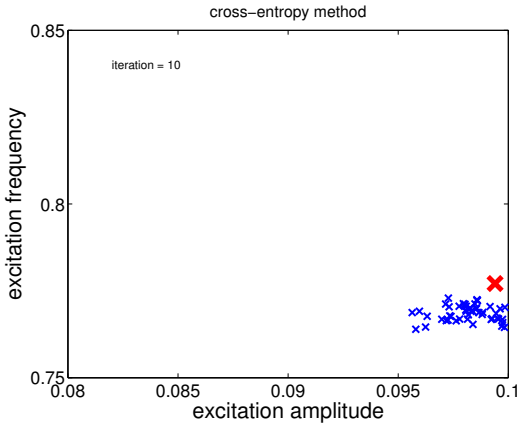

(d) $t = 10$

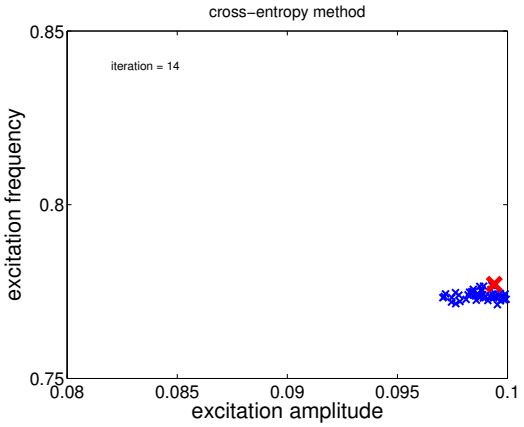

(e) $t = 14$

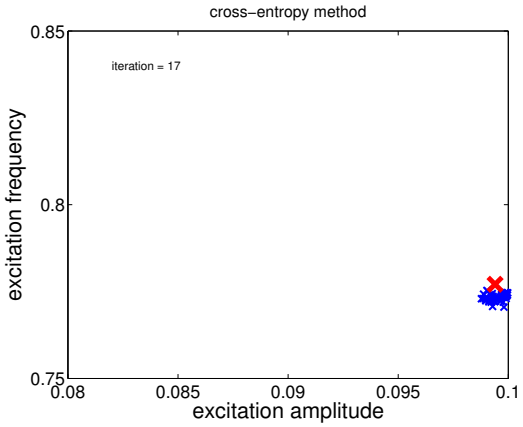

(f) $t = 17$

Figure 5. Illustration of CE method sampling of the domain at different levels (iterations) of the algorithm. The reference solution is indicated with a red cross.

Table 3. Evolution of CE algorithm using $N^s = 75$ samples.

level	P	μ_f	μ_Ω	σ_f	σ_Ω
01	+6.7650E-03	+9.0390E-02	+7.8364E-01	2.3783E-02	1.1257E-01
02	+6.9438E-03	+9.1348E-02	+7.8555E-01	1.0521E-02	5.5513E-02
03	+6.7726E-03	+9.1464E-02	+7.7791E-01	7.5571E-03	2.9343E-02
04	-7.8780E+00	+9.1598E-02	+7.7091E-01	5.8727E-03	2.2736E-02
05	+5.8535E-03	+9.1685E-02	+7.6281E-01	5.0653E-03	1.2983E-02
06	+1.8206E-01	+9.4203E-02	+7.6179E-01	5.1119E-03	1.1403E-02
07	+3.3294E-01	+9.7038E-02	+7.6184E-01	3.3773E-03	9.0893E-03
08	+3.3606E-01	+9.8348E-02	+7.6411E-01	2.6179E-03	6.5240E-03
09	+3.3771E-01	+9.8801E-02	+7.6678E-01	2.0570E-03	4.7431E-03
10	+3.3819E-01	+9.9067E-02	+7.6827E-01	1.5750E-03	4.0090E-03
11	+3.3835E-01	+9.8973E-02	+7.6836E-01	1.3353E-03	3.1594E-03
12	+3.3876E-01	+9.8813E-02	+7.6952E-01	1.1948E-03	2.7555E-03
13	+3.4010E-01	+9.9256E-02	+7.7121E-01	9.7802E-04	2.6319E-03
14	+3.4006E-01	+9.9392E-02	+7.7147E-01	8.1485E-04	2.3789E-03
15	+3.4082E-01	+9.9531E-02	+7.7219E-01	7.3002E-04	2.0875E-03
16	+3.4101E-01	+9.9467E-02	+7.7254E-01	6.7506E-04	1.8089E-03
17	+3.4122E-01	+9.9414E-02	+7.7329E-01	6.2117E-04	1.7465E-03
18	+3.4140E-01	+9.9319E-02	+7.7316E-01	5.5171E-04	1.5843E-03
19	+3.4166E-01	+9.9305E-02	+7.7362E-01	5.0059E-04	1.5502E-03
20	+3.4114E-01	+9.9474E-02	+7.7355E-01	4.4729E-04	1.4977E-03
21	+3.4193E-01	+9.9641E-02	+7.7385E-01	4.0136E-04	1.4061E-03
22	+3.4034E-01	+9.9626E-02	+7.7375E-01	3.8697E-04	1.4823E-03
23	+3.4093E-01	+9.9575E-02	+7.7368E-01	3.6392E-04	1.4292E-03
24	+3.4154E-01	+9.9508E-02	+7.7389E-01	3.5728E-04	1.3241E-03
25	+3.4193E-01	+9.9579E-02	+7.7427E-01	3.3566E-04	1.1937E-03
26	+3.4227E-01	+9.9599E-02	+7.7479E-01	3.2612E-04	1.1032E-03
27	+3.4203E-01	+9.9635E-02	+7.7490E-01	3.1476E-04	1.0496E-03
28	+3.4220E-01	+9.9731E-02	+7.7502E-01	2.9389E-04	1.0068E-03
29	+3.4203E-01	+9.9729E-02	+7.7487E-01	2.7659E-04	9.5792E-04

5 CONCLUDING REMARKS

This work presented the formulation of a nonlinear optimization problem to maximize the efficiency of a bi-stable energy harvesting device. Since the problem has jump-type discontinuities, which prevents the use of gradient-based methods, a stochastic approach based on the cross-entropy method was proposed to construct a numerical solution. Tests to verify the efficiency and accuracy of this approach were conducted, showing that the proposed algorithm is quite robust and effective.

Table 4. Evolution of CE algorithm using $N^s = 25$ samples.

level	P	μ_f	μ_Ω	σ_f	σ_Ω
01	-1.7354E-02	+9.2528E-02	+7.8304E-01	2.4005E-02	1.0592E-01
02	-1.7171E+00	+8.6541E-02	+7.7635E-01	9.5138E-03	3.8666E-02
03	+5.3859E-03	+8.8943E-02	+7.6449E-01	8.4947E-03	1.5642E-02
04	+7.8101E-03	+9.3665E-02	+7.5846E-01	4.9188E-03	9.0354E-03
05	+3.3423E-01	+9.6984E-02	+7.6137E-01	3.5145E-03	6.7145E-03
06	+3.3689E-01	+9.7425E-02	+7.6432E-01	2.2768E-03	4.5096E-03
07	+3.3610E-01	+9.7655E-02	+7.6447E-01	2.1021E-03	3.1061E-03
08	+3.3809E-01	+9.8104E-02	+7.6732E-01	1.9404E-03	2.4416E-03
09	+3.3903E-01	+9.8507E-02	+7.6834E-01	1.4161E-03	1.7015E-03
10	+3.3874E-01	+9.8577E-02	+7.6807E-01	1.3770E-03	1.2993E-03
11	+3.3924E-01	+9.9077E-02	+7.6836E-01	1.1700E-03	1.1012E-03
12	+3.3892E-01	+9.8925E-02	+7.6867E-01	1.1089E-03	1.0429E-03
13	+3.3937E-01	+9.8949E-02	+7.6930E-01	1.1003E-03	1.0517E-03
14	+3.3924E-01	+9.9278E-02	+7.6928E-01	1.0300E-03	8.6947E-04
15	+3.4030E-01	+9.9359E-02	+7.7019E-01	8.6681E-04	6.7889E-04

ACKNOWLEDGMENTS

The author is indebted to the Brazilian agencies CNPq, CAPES, and FAPERJ for the financial support given to this research. For the fruitful discussions about the optimization problem addressed in this work, he is also very grateful to Prof. Welington Oliveira (UERJ).

REFERENCES

Bernardini, D. and Litak, G. (2016). "An overview of 0–1 test for chaos." *Journal of the Brazilian Society of Mechanical Sciences and Engineering*, 38, 1433–1450.

Bhatti, N. A., Alizai, M. H., Syed, A. A., and L, M. (2016). "Energy harvesting and wireless transfer in sensor network applications: Concepts and experiences." *ACM Transactions on Sensor Networks*, 12, 24:1–24:40.

Cunha Jr, A., Nasser, R., Sampaio, R., Lopes, H., and Breitman, K. (2014). "Uncertainty quantification through Monte Carlo method in a cloud computing setting." *Computer Physics Communications*, 185, 1355–1363.

De Boer, P., Kroese, D. P., Mannor, S., and Rubinstein, R. Y. (2005). "A tutorial on the cross-entropy method." *Annals of Operations Research*, 134, 19–67.

Erturk, A., Hoffmann, J., and Inman, D. J. (2009). "A piezomagnetoelastic structure for broadband vibration energy harvesting." *Applied Physics Letters*, 94, 254102.

Gottwald, G. A. and Melbourne, I. (2004). "A new test for chaos in deterministic systems." *Proceedings of the Royal Society of London. Series A*, 460, 603–611.

Gottwald, G. A. and Melbourne, I. (2009a). "On the implementation of the 0-1 test for chaos." *SIAM Journal on Applied Dynamical Systems*, 8, 129–145.

Gottwald, G. A. and Melbourne, I. (2009b). "On the validity of the 0-1 test for chaos." *Nonlinearity*, 22, 1367–1382.

Gottwald, G. A. and Melbourne, I. (2016). *The 0-1 Test for Chaos: A review*, Vol. 915. Springer.

Harne, R. L. (2012). "Theoretical investigations of energy harvesting efficiency from structural vibrations using piezoelectric and electromagnetic oscillators." *The Journal of the Acoustical Society of America*, 132, 162–172.

Kroese, D. P., Rubinstein, R. Y., Cohen, I., Porotsky, S., and Taimre, T. (2013). *Cross-Entropy Method*. Springer, 326–333.

Kroese, D. P., Taimre, T., and Botev, Z. I. (2011). *Handbook of Monte Carlo Methods*. Wiley.

Lopes, V. G., Peterson, J. V. L. L., and Jr, A. C. (2017). "Numerical study of parameters influence over the dynamics of a piezo-magneto-elastic energy harvesting device." *XXXVII Congresso Nacional de Matemática Aplicada e Computacional (CNMAC 2017)*, São José dos Campos, Brazil.

Nabavi, S. and Zhang, L. (2016). "MEMS piezoelectric energy harvester design and optimization based on Genetic Algorithm." *2016 IEEE International Ultrasonics Symposium (IUS)*, 1–4.

Peterson, J. V. L. L., Lopes, V. G., and Cunha Jr, A. (2016). "Maximization of the electrical power generated by a piezo-magneto-elastic energy harvesting device." *XXXVI Congresso Nacional de Matemática Aplicada e Computacional*, Gramado, Brazil.

Pfenniger, A., Stahel, A., Koch, V. M., Obrist, D., and Vogel, R. (2014). "Energy harvesting through arterial wall deformation: A FEM approach to fluid–structure interactions and magneto-hydrodynamics." *Applied Mathematical Modelling*, 38, 3325–3338.

Priya, S. and Inman, D. J. (2009). *Energy Harvesting Technologies*. Springer.

Rechenbach, B., Willatzen, M., and Lassen, B. (2016). "Theoretical study of the electromechanical efficiency of a loaded tubular dielectric elastomer actuator." *Applied Mathematical Modelling*, 40, 1232–1246.

Rubinstein, R. Y. (1997). "Optimization of computer simulation models with rare events." *European Journal of Operations Research*, 99, 89–112.

Rubinstein, R. Y. and Kroese, D. P. (2004). *The Cross-Entropy Method: A Unified Approach to Combinatorial Optimization, Monte-Carlo Simulation and Machine Learning*. Information Science and Statistics. Springer-Verlag.

Rubinstein, R. Y. and Kroese, D. P. (2016). *Simulation and the Monte Carlo Method*. Wiley Series in Probability and Statistics. Wiley, 3rd edition.

Selvan, K. V. and Ali, M. S. M. (2016). "Micro-scale energy harvesting devices: Review of methodological performances in the last decade." *Renewable and Sustainable Energy Reviews*, 54, 1035–1047.

Spies, P., Pollak, M., and Mateu, L. (2015). *Handbook of Energy Harvesting Power Supplies and Applications*. Pan Stanford.

Ying, Q., Yuan, W., and Hu, N. (2015). "Improving the efficiency of harvesting electricity from living trees." *Journal of Renewable and Sustainable Energy*, 7.